

# Substrate-induced magnetic ordering and switching of iron porphyrin molecules

H. WENDE<sup>1\*</sup>†‡, M. BERNIEN<sup>1</sup>, J. LUO<sup>1</sup>, C. SORG<sup>1</sup>, N. PONPANDIAN<sup>1</sup>, J. KURDE<sup>1</sup>, J. MIGUEL<sup>1</sup>, M. PIANTEK<sup>1</sup>, X. XU<sup>1</sup>, PH. ECKHOLD<sup>1</sup>, W. KUCH<sup>1</sup>, K. BABERSCHKE<sup>1</sup>, P. M. PANCHMATIA<sup>2†</sup>, B. SANYAL<sup>2</sup>, P. M. OPPENEER<sup>2</sup> AND O. ERIKSSON<sup>2</sup>

<sup>1</sup>Institut für Experimentalphysik, Freie Universität Berlin, Arnimallee 14, D-14195 Berlin-Dahlem, Germany

<sup>2</sup>Department of Physics, Uppsala University, Box 530, S-751 21 Uppsala, Sweden

\*Present address: Universität Duisburg-Essen, Fachbereich Physik, Experimentalphysik – AG Wende, Lotharstr. 1, D-47048 Duisburg, Germany

†These authors contributed equally to this work

‡e-mail: heiko.wende@uni-due.de

Published online: 10 June 2007; doi:10.1038/nmat1932

To realize molecular spintronic devices, it is important to externally control the magnetization of a molecular magnet. One class of materials particularly promising as building blocks for molecular electronic devices is the paramagnetic porphyrin molecule in contact with a metallic substrate. Here, we study the structural orientation and the magnetic coupling of *in-situ*-sublimated Fe porphyrin molecules on ferromagnetic Ni and Co films on Cu(100). Our studies involve X-ray absorption spectroscopy and X-ray magnetic circular dichroism experiments. In a combined experimental and computational study we demonstrate that owing to an indirect, superexchange interaction between Fe atoms in the molecules and atoms in the substrate (Co or Ni) the paramagnetic molecules can be made to order ferromagnetically. The Fe magnetic moment can be rotated along directions in plane as well as out of plane by a magnetization reversal of the substrate, thereby opening up an avenue for spin-dependent molecular electronics.

The porphyrin molecule is an archetypal metallorganic complex, which shows up in many biochemical molecules like chlorophyll, haemoglobin and cytochrome. Probable usage of these molecules in various applications like optical switches, information storage and nonlinear optics is reported in the literature<sup>1–3</sup>. The prospect of switching the spin in the metalloporphyrin ring is a particularly interesting one, as this could be used, for example, for spin-dependent electric transport through biomolecular devices. Previously, the magnetic and structural properties of porphyrin molecules in bulk and on surfaces have been studied by various techniques, such as temperature-dependent susceptibility<sup>4</sup>, nuclear magnetic resonance and X-ray diffraction<sup>5</sup> and X-ray photoelectron spectroscopy<sup>6</sup> as well as X-ray absorption spectroscopy (XAS)<sup>7–11</sup>. Also, electronic-structure calculations have been carried out for free molecules<sup>12,13</sup>.

Here we investigate *in-situ*-prepared monolayer (ML) and submonolayer coverages of octaethylporphyrin Fe(III) chloride (OEP) on 5 ML Co/Cu(100) and 15 ML Ni/Cu(100). By using these thicknesses of the ferromagnetic films the easy axis of magnetization can be tuned from in plane (Co) to out of plane (Ni). For the adsorbed Fe OEP molecules we study the structural orientation, the electronic structure and, most importantly, the magnetic properties and exchange coupling between molecules and the ferromagnetic films. This is achieved by XAS<sup>14</sup> and X-ray magnetic circular dichroism (XMCD) measurements<sup>15</sup> in combination with theoretical calculations of the electronic structure and magnetic exchange coupling.

Our first aim is to assess the orientation of the Fe OEP molecules on the surfaces and whether these stay intact when sublimated on the substrate. The molecular orientation is

investigated here by angle-dependent near-edge X-ray absorption fine-structure (NEXAFS) spectra<sup>16</sup> measured at the N and K edges for both ferromagnetic substrates (Co, Ni) presented in Fig. 1 and in the Supplementary Information, respectively. In Fig. 1 the geometry of the porphyrin molecule with a quasi-planar central part (Fe–N–C bonds) and the end groups is also shown. The comparison of the spectra at the N K edge reveals the same fine structures for the Co and Ni substrates and hence indicates a very similar adsorption geometry. Clear  $\sigma^*$  and  $\pi^*$  resonances can be identified, which show a distinct angular dependence. The detailed NEXAFS analysis (see the Supplementary Information) reveals that the plane of the four nitrogen atoms is aligned parallel to the surface. Furthermore, the N K-edge fine structure (Fig. 1) is also a sensitive indicator that the porphyrin part of the molecule is intact on the surface: The spectra show all fine structures discussed in ref. 10 for a similar molecule: Zn tetraphenylporphyrin (ZnTPP). If the central  $3d$  atom is missing, a third peak is expected at about 403.0 eV. Because this feature is missing from our spectra, we can conclude that the Fe atom is located in the molecule.

Now we turn to the analysis of the element-specific magnetic properties by investigating the XMCD spectra presented in Fig. 2. The spectra are shown at the  $L_{2,3}$  edges of Fe for both ferromagnetic Co and Ni substrates at 300 K in an applied magnetic field of 10 mT. Although the coverage of 1 ML of porphyrin molecules corresponds to an effective Fe coverage in the 1/100 ML regime, the XMCD spectra are nearly free of noise, owing to the high photon brilliance. Because the easy axis of magnetization is out of plane for Ni and in plane for Co ([110] direction), the measurements were made at normal and at grazing incidence, respectively. The energy positions of the Fe  $L_{2,3}$  edges are close to the ones reported for Fe(II) (see for

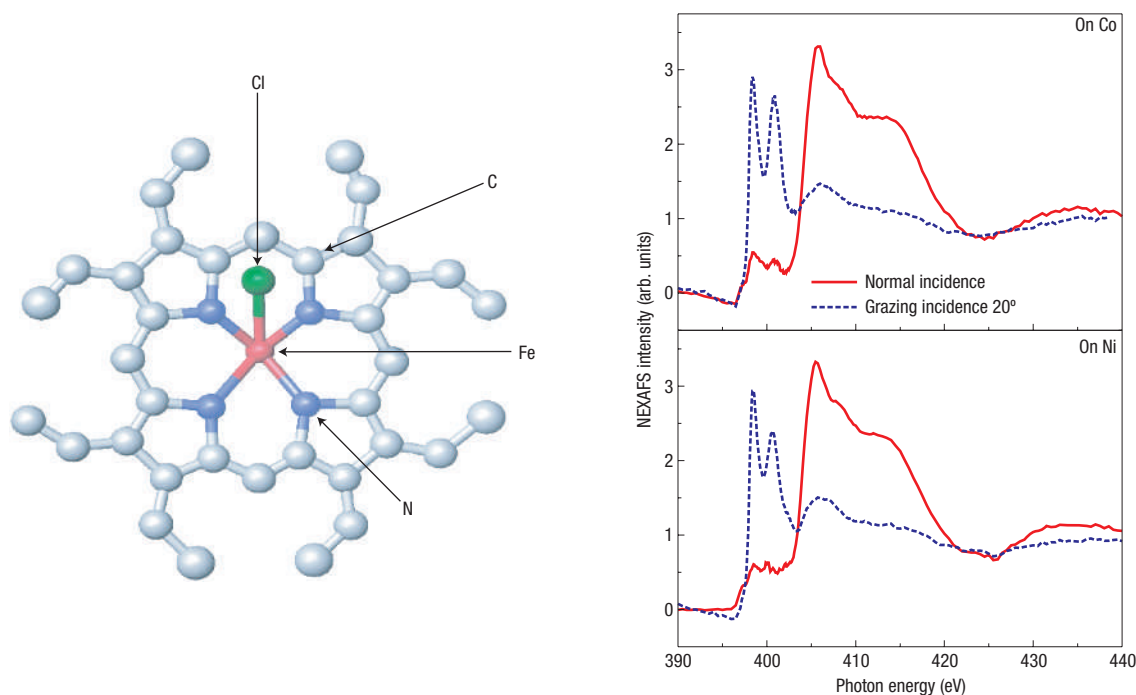


**Figure 1** The Fe octaethylporphyrin (OEP) chloride molecule and the structural orientation of Fe OEP determined by NEXAFS spectroscopy. Left: Schematic illustration of Fe OEP chloride molecule. Right: Angular dependence of NEXAFS (linear polarization) of Fe OEP at the Ni K edge for the Co and Ni substrates. X-rays at normal and grazing incidence ( $20^\circ$ ) were applied to determine the molecule's orientation.

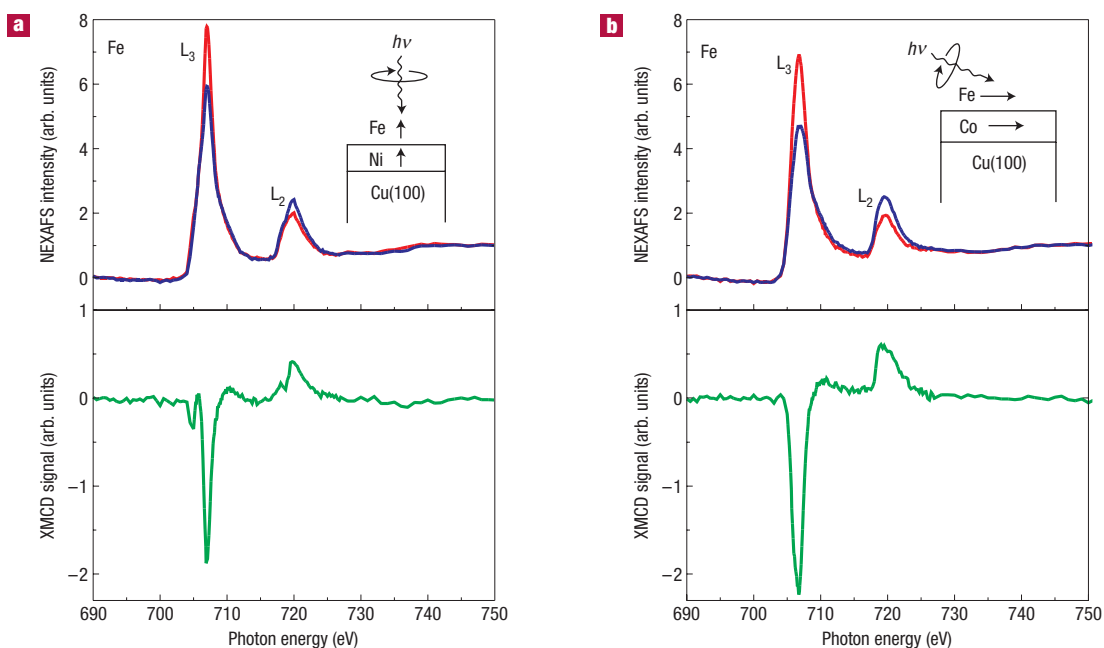


**Figure 2** Element-specific magnetic properties of the Fe OEP molecule on ferromagnetic substrates determined by XMCD. **a, b**, X-ray absorption coefficients for right and left circularly polarized X-rays  $\mu^+(E)$  (red) and  $\mu^-(E)$  (blue) (top) and XMCD (bottom) of the central Fe atom of the OEP molecule on Ni (**a**) and Co (**b**) substrates (300 K, 10 mT). The insets depict the orientation of the sample to the incident X-rays. The arrows for Fe and the ferromagnetic films show the alignments of the spins.

example refs 17,18). This indicates that Cl is not present at the time of the measurement. Furthermore, our spectra show similar line shapes at the Fe  $L_{2,3}$  edges to the ones published in ref. 18 for Fe(II) in haem molecules. To substantiate these observations we

investigated the X-ray absorption coefficient in the vicinity of the Cl  $L_{2,3}$  edges. As expected, no Cl signal could be detected.

The XMCD signals in Fig. 2 reveal that by adsorption of paramagnetic porphyrin molecules on the ferromagnetic film the

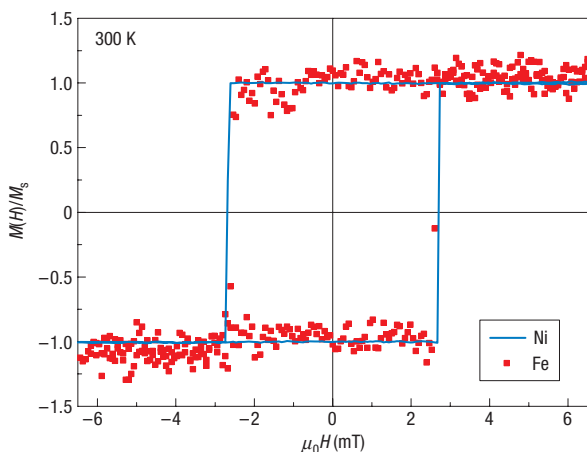


**Figure 3** The element-specific field dependence of the magnetization of the Fe atoms in the molecule and the ferromagnetic substrate (Ni). Hysteresis curves of the Fe atom (filled squares) and Ni (full line) obtained by the  $L_3$  edge XMCD maxima of Fe OEP on Ni/Cu(100) at 300 K.

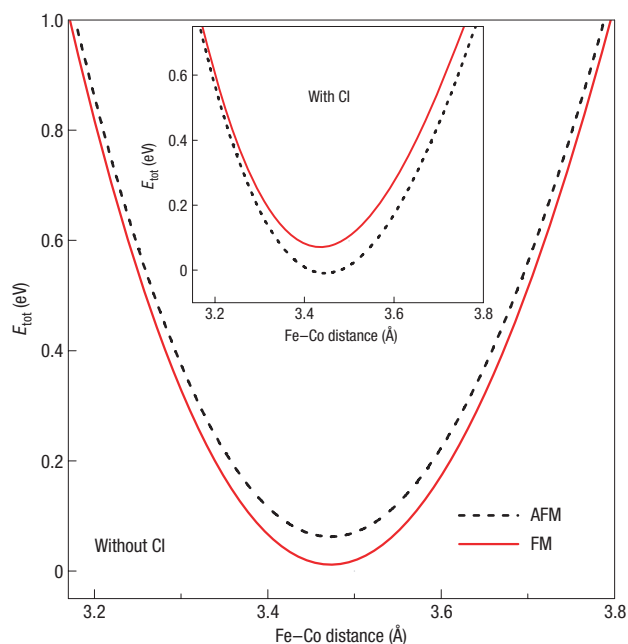


**Figure 4** Computed total energies as a function of the distance of the Fe porphyrin from the Co substrate, for parallel (FM) and antiparallel (AFM) alignments of Fe and Co spins. The Fe–Co distance is defined as the distance of Fe from the nearest top-layer Co atom. GGA +  $U$  total energies (with  $U = 4$  eV) are shown for de-chlorinated Fe porphyrin, whereas those of the chlorine-ligated Fe porphyrin are shown in the inset.

molecules are not only structurally but also magnetically ordered. In Fig. 2 the XMCD signals are negative at the  $L_3$  edge (as are the Co and Ni XMCD signals), which demonstrates that the coupling of the molecules to the films is ferromagnetic. An analysis of the absorption coefficients for right and left circularly polarized X-rays,  $\mu^+(E)$  and  $\mu^-(E)$ , respectively, shows that the linewidth for the experiment on the Ni substrate is sharper (Fig. 2a top) as compared

to that of the Co substrate (Fig. 2b top). This feature is connected to the pronounced double structure in the Fe XMCD for the Ni substrate (Fig. 2a bottom) in comparison to the broader XMCD for the Co substrate. The origin of these variations is the different Fe orbitals being probed at the respective incidences: at normal incidence we are investigating the unoccupied Fe orbitals in plane, whereas at grazing incidence it is partly the out-of-plane orbitals that are measured. The XMCD spectrum at grazing incidence for Fe OEP on a double layer consisting of a 5 ML Ni film on a 6 ML Co film, a substrate that has the magnetization in plane, reveals the same broad dichroic spectrum as seen for porphyrins on a Co substrate (Fig. 2b bottom), which also shows an in-plane magnetization. The fact that different substrates result in similar dichroic spectra demonstrates that the XMCD fine structure seen in Fig. 2a reflects the magnetization of the Fe orbitals being probed.

To achieve further insight into the magnetic coupling of the porphyrin molecules to the ferromagnetic films, we measured element-specific hysteresis loops as presented in Fig. 3 for the Ni film substrate at 300 K. The field-dependent Fe and Ni  $L_3$  XMCD intensities are shown at fixed photon energy. The signals are normalized according to the saturation values. It is clear that the two hysteresis loops coincide. Hence, the orientation of the Fe spin switches in the same way as the spins of the ferromagnetic film. This demonstrates the central result of our study: the presence of a substantial ferromagnetic exchange coupling of the Fe moments of planar oriented porphyrin molecules to a magnetic substrate.

To unravel the nature of the exceptional magnetic coupling we carried out density-functional-theory-based electronic-structure calculations for porphyrin molecules on a magnetic substrate. Specifically, we have investigated both chlorine-ligated and unligated iron porphyrin rings on an f.c.c. Co(100) substrate. Our self-consistent calculations have been carried out using a full-potential code, in which the generalized gradient approximation (GGA)<sup>19</sup> has been adopted for the exchange–correlation functional. To treat strong electron interactions beyond those present in the DFT-GGA functional, we have also used the GGA +  $U$  approach, in which an additional on-site Hubbard- $U$  term is included on the iron atom. From GGA +  $U$  calculations for free-standing porphyrin molecules similar to the ones studied here, we found that a  $U$  value of 4 eV and an exchange parameter  $J$  of 1 eV provided the best results. These values of  $U$  and  $J$  predict—for free molecules—a low  $S = 1$  spin state for the unligated molecule (that is, Fe(II)) and a high  $S = 5/2$  spin state for the Cl ligated molecule (corresponding to Fe(III)).

The total energy of the system was calculated as a function of the vertical distance  $d$  between the porphyrin molecule and substrate, measured as the distance between the iron atom and the nearest, top-layer Co atom for both the ferromagnetic (FM) and antiferromagnetic (AFM) alignment of the Fe and Co spins. Figure 4 shows the computed total energies as a function of the distance  $d$ . The depicted total energies have been shifted to zero value by subtraction of the lowest total-energy value. The Cl atom of the chlorine-ligated porphyrin molecule was placed at the known<sup>7</sup> experimental distance of 2.16 Å from the Fe atom, pointing away from the surface. The optimal Fe–Co distance is computed to be 3.4–3.5 Å, for both the Cl-ligated and unligated molecules; this value is obtained with the GGA as well as the GGA +  $U$  approach. A clear difference between the chlorine-ligated and unligated molecules is calculated for the magnetic coupling of the Fe atom to the Co substrate: the chlorine-ligated porphyrin prefers the AFM coupling to the Co surface, as is given by both GGA and GGA +  $U$  calculations. For the non-ligated molecule the situation is reversed: here the FM coupling between Fe and Co spin moments is clearly preferred (see Fig. 4), from both GGA and GGA +  $U$  approaches. The AFM orientation computed for the chlorine-ligated system

obviously does not tally with the experimental observation. In contrast, the unligated porphyrin molecule shows a clear preference for the FM state. Hence, according to our calculations the Cl atom is evidently not present on the porphyrin molecule when adsorbed on the substrate.

A first understanding of how the exchange coupling between Fe and Co takes place can be collected from the partial densities of states (DOSs). Figure 5 shows the spin-resolved, partial DOSs for the unligated system, computed with the GGA +  $U$  approach. These DOSs were computed for both the FM and AFM alignments, at the optimal Fe–Co distance of 3.5 Å. We note that whereas our GGA and GGA +  $U$  calculations provide the same trend in preferred magnetic orientation and for the equilibrium Fe–Co distance, the addition of the Coulomb  $U$  modifies the energy positions of the Fe 3*d* states, and consequently the corresponding DOS. Figure 5 illustrates that there exists an Fe–N hybridization, as can be recognized from the occurrence of DOS peaks at the same energies for Fe 3*d* and N 2*p* states (indicated by vertical bars). These N DOS peaks, moreover, follow the Fe 3*d* spin polarization, as they reverse on changing the Fe spin direction from FM to AFM. No such clear hybridization between Fe and Co can be observed. This is consistent with the Fe–Co distance of 3.5 Å, which is sufficiently large to prevent a direct overlap of Fe and Co *d* orbitals. A small Co–N hybridization, however, can be deduced from the N and Co partial DOSs at 2.6–3 eV binding energy. This shows that the chemical binding of the porphyrin to the substrate primarily takes place between the C and N atoms of the porphyrin and the Co atoms of the substrate, which provides a sufficiently strong chemical bond. The strength of the binding of the whole molecule to the Co substrate is calculated to be several electronvolts (see Fig. 4). The use of a Co substrate hence provides a chemical bonding distinct from that observed for example in studies using Au substrates<sup>20,21</sup>.

Deeper insight into the mechanism of the Fe–Co exchange coupling can be obtained from an analysis of charge and magnetization densities. Calculated charge densities confirm the conclusions drawn from the DOS plots, that is, these demonstrate the absence of a direct hybridization between Fe and Co orbitals. An energy-resolved analysis of the charge densities showed, furthermore, that the Fe–N bonding occurring at about 2.5 eV binding energy is due to  $\pi$  bonding of Fe  $d_{xz}$ ,  $d_{yz}$  and N  $p_z$  orbitals. Figure 6 shows the GGA +  $U$  computed magnetization density of the unligated molecule, ferromagnetically coupled to the Co substrate. Magnetization densities are prominently seen around Fe and Co atoms, whereas a vanishingly small magnetization density exists in between. Conversely, the nitrogen atoms reveal a magnetization density extending towards the Co substrate, hence providing evidence for a spin polarization of the N through bonding to the Co atoms. As a result, the spin moment of the whole porphyrin molecule increases slightly from 2.00  $\mu_B$  for the free molecule to 2.17  $\mu_B$  for the deposited molecule. The Fe(II) oxidation state is therefore not changed on adsorption. However, there is also a small spin polarization on some C atoms, without any direct bonding to the Fe atom. Our calculations exclude a direct exchange between Fe and Co. Instead, we identify a 90° ferromagnetic indirect exchange mechanism as the reason for the FM coupling between Fe and Co, a finding that is in accordance with the Kanamori–Goodenough rules for superexchange<sup>22</sup>. This indirect exchange coupling is mediated through the nitrogen atoms, where the weak bonding of Co and N provides exchange splitting of the  $p_z$  orbitals of the four N atoms. The latter are in turn hybridized with the exchange-split Fe  $d_{xz}$  orbitals and an effective stabilization of the parallel alignment results. The energy difference between FM and AFM orientations is small, but it is correctly given by our *ab initio* calculations.

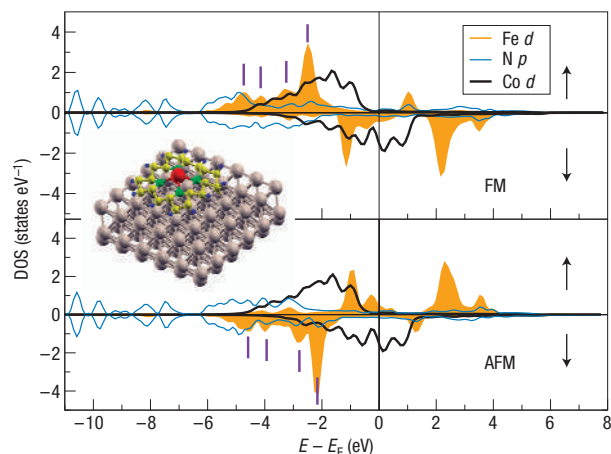


**Figure 5** Calculated GGA +  $U$  partial DOS of the iron porphyrin (without chlorine) on a Co substrate, for  $d = 3.5$  Å. The spin-resolved partial DOS is shown for parallel (FM) and antiparallel (AFM) alignment, respectively, of Fe and Co spins. Positive partial DOS corresponds to spin up, negative partial DOS to spin down. Vertical bars indicate common Fe and N partial DOS peaks. The inset shows a three-dimensional visualization of the molecule on the substrate (in the calculations a larger unit cell than shown was used).

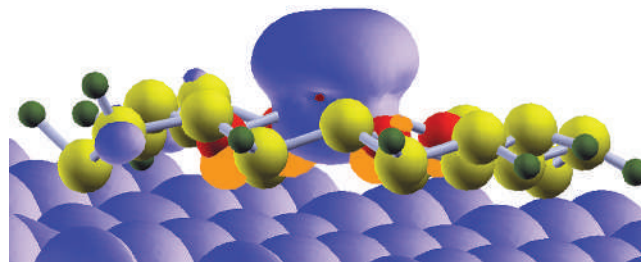


**Figure 6** Magnetization density calculated with the GGA +  $U$  approach for the unligated molecule, for the FM orientation of Fe and Co spins. The magnetization density iso-surfaces around the Fe and Co atoms are shown in blue (atom positions: C, yellow; H, dark green; N, red). The four nitrogen atoms are spin polarized towards the Co surface, as is shown by the orange-coloured magnetization densities extending to the surface.

## METHODS

The XAS measurements were carried out on *in situ* prepared samples at the UE56/2-PGM2 beamline at BESSY. The NEXAFS and XMCD data were recorded using total electron yield by measuring the drain current. The self-consistent *ab initio* calculations have been carried out using the full-potential, plane-wave code VASP, based on the projector augmented wave method<sup>23–25</sup>. In our calculations we used the experimental geometry of the Fe porphyrin molecule, available in the literature<sup>7</sup>. For further details on the experimental and theoretical techniques, see Supplementary Information.

Received 27 December 2006; accepted 18 April 2007; published 10 June 2007.

## References

- Karki, L. *et al.* Electronic Stark effect studies of a porphyrin-based push–pull chromophore displaying a large first hyperpolarizability: State-specific contributions to  $\beta$ . *J. Am. Chem. Soc.* **120**, 2606–2611 (1998).
- LeCours, S. M. *et al.* Push–pull arylethynyl porphyrins: New chromophores that exhibit large molecular first-order hyperpolarizabilities. *J. Am. Chem. Soc.* **118**, 1497–1503 (1996).
- Barth, J. V., Costantini, G. & Kern, K. Engineering atomic and molecular nanostructures at surfaces. *Nature* **437**, 671–679 (2005).
- Maricondi, C., Swift, W. & Straub, D. K. Thermomagnetic analysis of hemin and related compounds. *J. Am. Chem. Soc.* **91**, 5205–5210 (1969).

5. Kalish, H. *et al.* Meso substituent effects on the geometric and electronic structures of high-spin and low-spin iron(III) complexes of mono-meso-substituted octaethylporphyrins. *Inorg. Chem.* **41**, 989–997 (2002).
6. Gottfried, J. M., Flechtner, K., Kretschmann, A., Lukaszczk, T. & Steinrück, H.-P. Direct synthesis of a metalloporphyrin complex on a surface. *J. Am. Chem. Soc.* **128**, 5644–5645 (2006).
7. Goulon, J., Goulon-Ginet, Ch. & Gotte, V. in *The Porphyrin Handbook* Vol. 7 (eds Kadish, K. M., Smith, K. M. & Guillard, R.) (Academic, New York, 2000).
8. Okajima, T., Yamamoto, Y., Ouchi, Y. & Seki, K. NEXAFS spectra of metalotetraphenylporphyrins with adsorbed nitrogen monoxide. *J. Electron. Spectroscop. Relat. Phenom.* **114–116**, 849–854 (2001).
9. Polzonetti, G. *et al.* Electronic structure of platinum complex-Zn-porphyrinato assembled macrosystems, related precursors and model molecules, as probed by X-ray absorption spectroscopy (NEXAFS): Theory and experiment. *Chem. Phys.* **296**, 87–100 (2004).
10. Narioka, S. *et al.* XANES spectroscopic studies of evaporated porphyrin films: Molecular orientation and electronic structure. *J. Phys. Chem.* **99**, 1332–1337 (1995).
11. Scheybal, A. *et al.* Induced magnetic ordering in a molecular monolayer. *Chem. Phys. Lett.* **411**, 214–220 (2005).
12. Ghosh, A., Gonzalez, E., Vangberg, T. & Taylor, P. Molecular structures and electron distributions of higher-valent iron and manganese porphyrins. Density functional theory calculations and some preliminary open-shell coupled-cluster results. *J. Porphyrins Phthalocyanines* **5**, 345–356 (2001).
13. Liao, M.-S. & Scheiner, S. Electronic structure and bonding in unligated and ligated FeII porphyrins. *J. Chem. Phys.* **116**, 3635–3645 (2002).
14. Stöhr, J. *et al.* Liquid crystal alignment on carbonaceous surfaces with orientational order. *Science* **292**, 2299–2302 (2001).
15. Wende, H. Recent advances in X-ray absorption spectroscopy. *Rep. Prog. Phys.* **67**, 2105–2181 (2004).
16. Stöhr, J. *NEXAFS Spectroscopy* (Springer, Berlin, 1992).
17. Heijboer, W. M. *et al.* In-situ soft X-ray absorption of over-exchanged Fe/ZSM5. *J. Phys. Chem. B* **107**, 13069–13075 (2003).
18. Hocking, R. K. *et al.* Fe L-edge X-ray absorption spectroscopy of low-spin heme relative to non-heme FE complexes: Delocalization of Fe d-electrons into the porphyrin ligand. *J. Am. Chem. Soc.* **129**, 113–125 (2007).
19. Perdew, J. P. & Wang, Y. Accurate and simple analytic representation of the electron-gas correlation energy. *Phys. Rev. B* **45**, 13244–13249 (1992).
20. Barlow, D. E., Scudiero, L. & Hipps, K. W. Scanning tunneling microscopy study of the structure and orbital-mediated tunneling spectra of cobalt(II) phthalocyanine and cobalt(II) tetraphenylporphyrin on Au(111): Mixed composition films. *Langmuir* **20**, 4413–4421 (2004).
21. Leung, K. *et al.* Density functional theory and DFT + *U* study of transition metal porphine on Au(111) surfaces and effects of applied electric fields. *J. Am. Chem. Phys. Soc.* **128**, 3659–3668 (2006).
22. Goodenough, J. B. *Magnetism and the Chemical Bond* (Wiley, New York, 1963).
23. Kresse, G. & Hafner, J. Ab initio molecular dynamics for liquid metals. *Phys. Rev. B* **47**, 558–561 (1993).
24. Kresse, G. & Furthmüller, J. Efficient iterative schemes for ab initio total-energy calculations using a plane-wave basis set. *Phys. Rev. B* **54**, 11169–11186 (1996).
25. Blöchl, P. E. Projector augmented-wave method. *Phys. Rev. B* **50**, 17953–17979 (1994).

#### Acknowledgements

Support by the BMBF (05 KS4 KEB/5), the DFG (Sfb658), the Swedish Research Council, the Foundation for Strategic Research and the Swedish National Infrastructure for Computing (SNIC) is gratefully acknowledged. One of us (H.W.) wishes to thank the DFG (Heisenberg fellowship) and Center for Dynamical Studies, Uppsala University, for hospitality and support during his stay in Uppsala. P.M.P. and P.M.O. acknowledge support through the EU network on molecular biosensors (MOT-Test). We thank B. Zada, W. Mahler and F. Senf for technical help during the beamtime. Correspondence and requests for materials should be addressed to H.W. Supplementary Information accompanies this paper on [www.nature.com/naturematerials](http://www.nature.com/naturematerials).

#### Author contributions

The experimental investigation was carried out at the Freie Universität, Berlin, whereas the theoretical research was carried out at Uppsala University. Both groups contributed equally to the work.

#### Competing financial interests

The authors declare no competing financial interests.

Reprints and permission information is available online at <http://npg.nature.com/reprintsandpermissions/>